AIRFLOW REVERSALS IN HIGH-TEMPERATURE KILN DRYING OF *PINUS RADIATA* BOARDS. 1: DRYING OF A SINGLE BOARD

PANG SHUSHENG

New Zealand Forest Research Institute,
Private Bag 3020, Rotorua, New Zealand

R. B. KEEY

Department of Chemical and Process Engineering,
University of Canterbury, Christchurch, New Zealand

T. A. G. LANGRISH

Department of Chemical Engineering,
University of Sydney, New South Wales 2006, Australia

and J. C. F. WALKER

School of Forestry,
University of Canterbury, Christchurch, New Zealand

(Received for publication 30 June 1994; revision 30 September 1994)

ABSTRACT

Predictions of local temperature and moisture-content profiles in the high-temperature drying of single *Pinus radiata* D.Don boards of 100×50 mm, for both unidirectional flow of air and airflow reversals, have been based on a rigorous mathematical model. This was reviewed and confirmed in drying tests conducted at New Zealand Forest Research Institute (NZFRI). When the air flowed in one direction only, temperatures were higher and moisture contents were lower near the leading edge of the board than at other positions across the board, because of the decrease in heat- and mass-transfer coefficients with distance from the leading edge. These differences could be reduced, to a certain extent, by reversing the airflow, thus establishing more-uniform temperature and moisture-content profiles.

In the drying of a sapwood board using unidirectional airflow at dry-bulb/wet-bulb temperatures of 120°/70°C, the maximum moisture-content variation between the leading and trailing edges after 4 hours of drying was predicted to be 27% m.c. This variation persisted for about 6 to 8 hours, before decreasing with further drying. The largest difference in surface temperature (27°C) occurred between the same positions as for the moisture content after 6 hours of drying. With airflow reversals, the differences both in temperature and in moisture content were reduced, with the middle region

becoming the wettest during drying. Airflow reversals every 4 or 8 hours shortened the period of maximum moisture-content difference, but the peak value was not reduced. Reversing the airflow every 3 hours, or reversals after 2 and 6 hours, was more effective in reducing the greatest moisture-content difference to below 20%. All reversal strategies resulted in similar moisture-content and temperature profiles in the later period of drying (after 16 hours). For heartwood, the benefit of airflow reversals is not as significant as that for sapwood, since the differences in both temperature and moisture content with unidirectional airflow are smaller because of the much lower initial moisture content of heartwood.

Keywords: high-temperature drying; airflow reversals; moisture-content variations; *Pinus radiata.*

INTRODUCTION

High-temperature (HT) drying, involving air temperatures exceeding 100°C, is a commercially established technique which significantly reduces the drying time of softwood boards compared to that for a conventional drying schedule (Williams & Kininmonth 1984). High-temperature drying takes advantage of the much greater heat-transfer rates occurring with high-temperature schedules, typically 120°/70° or 140°/90°C. However, some drying-related defects, such as internal checking (Booker & Haslett 1993), may be associated with the faster drying using higher temperatures. In order to understand and hence to prevent drying defects, we need to describe the heat- and mass-transfer processes both within and outside timber boards.

The initial drying is particularly influenced by the external mass-transfer process of convection of vapour from the surface of the boards. Some experimental and theoretical studies have been carried out (Kho *et al.* 1989, 1990; Langrish *et al.* 1993) to investigate the variation in external mass-transfer coefficients with distance from the leading edge of each board within a stack. Kho *et al.* (1989, 1990) reported that experimentally measured profiles of the mass-transfer coefficients over each board in a stack within a small industrial kiln were not uniform both over a single board and across a kiln-stack; the values were higher than those over a sharp-edged flat plate.

Pang *et al.* (in press) have proposed a mathematical model to simulate the moisture-transfer process within wood, based on physiological features of green wood and observed behaviour during high-temperature drying. The model has been solved numerically to give the temperature and moisture-content profiles of a *Pinus radiata* board. Predictions of the model both for heartwood and for sapwood agree closely with independent measurements of temperatures found on drying a single board (W.Miller, I.Simpson pers. comm.).

In all of these previous studies, the air has been considered to flow in one direction only. However, in practical kiln operations, the airflow is reversed periodically to achieve more-uniform drying. Therefore, in this study we first tested the mathematical model against additional experimental results. Then the local temperature and moisture-content profiles across a board were calculated from this model both for unidirectional airflow and for airflow reversals. In the calculations, variations in local mass-transfer coefficients over a single board were taken into account. These predictions indicate the effects of airflow reversals for sapwood and heartwood in terms of moisture content and temperature uniformity within a board.

PROFILES OF HEAT- AND MASS-TRANSFER COEFFICIENTS IN AN AIRSTREAM

In the tests reported by Kho *et al.* (1989, 1990), a 100×25-mm truncated aluminium board coated with naphthalene was placed within a kiln stack, and the mass-transfer rate was determined by measuring the amount of sublimation from the surface. Experiments were carried out at air velocities of 3, 5, and 7 m/s respectively. The mass-transfer coefficient variations over the first five boards with distances measured from the leading edge of the first board are shown in Fig. 1, and some important features can be observed:

(a) The maximum mass-transfer coefficient occurs over the front of the first board 10–30 mm behind the leading edge;

(b) The maximum values over successive boards occur at positions close to leading edges of each board, then fall to an asymptotic value some 30–40 mm from the leading edge of each board;

(c) From the second board on in the airstream direction (with exception of the last board), the coefficient profiles over each board are essentially the same for a fixed air velocity, with higher values being observed for higher air velocities.

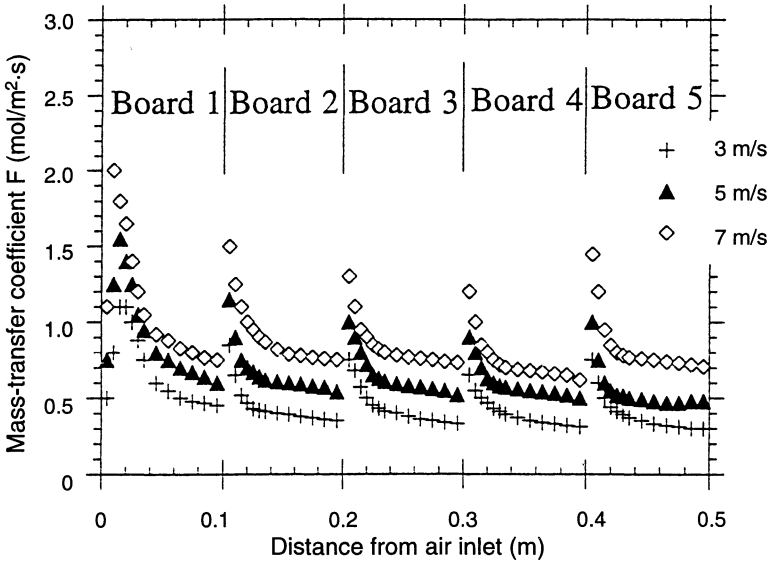

FIG. 1–Local mass-transfer coefficient variation with distance from the leading edge for the first five boards with normal board gap of 1 mm and uniform board level. Source: Kho *et al.* (1990).

In these experiments, the effects of minor board irregularities have also been investigated. With a 5-mm gap between adjacent boards, the local mass-transfer coefficient was enhanced about 20% compared to where the gap was only 1 mm. The influence of different heights of adjacent boards has been observed to change the local coefficients to a varying extent: a lower leading board has a greater influence on the front portion of the sample board than that of a lower trailing board with the same height difference. Significant enhanced local mass-transfer coefficients over the sample board were observed when the sample board was lower

than both adjacent ones. The asymptotic values of the mass-transfer coefficients are greater than those over sharp-edged flat plates, owing to the generation and diffusion of stationary eddies along the boards (Sørenson 1969; Miller 1972). These eddies have been observed by Lee (1990), using a smoke visualisation technique.

The flow over an array of slabs, similar in geometry to a stack of boards in a kiln, has been modelled using computational fluid dynamics (Langrish *et al.* 1993). By using the Reynolds analogy between skin friction and mass transfer from the surface, it is possible to compute local mass-transfer coefficients. The magnitude and variation of the calculated coefficients with distance are in good agreement with the experimental values, except that the enhancements at the leading edge of each board are under-predicted owing to inadequacies in modelling the flow at the leading edge.

The measured mass-transfer coefficient (F), which is based on the molar concentration difference, can be converted into one based on the vapour partial pressure difference (β). The latter will be used in the following simulation. The heat-transfer coefficient is calculated from Chilton-Colburn analogy, in which the radiative heat is taken into account (Pang 1994).

If the air flows in only one direction, the local mass- and heat-transfer rates are higher over the leading edge for a single board, thus the board surface-temperature is higher and the moisture content is lower than elsewhere across the board. These non-uniformities limit our ability to manipulate the external conditions which can be chosen to minimise degrade caused by excessive moisture-content maldistribution. In practice, somewhat more-uniform profiles of heat- and mass-transfer coefficients are created by reversing the airflow periodically. Under these conditions, the profiles of the heat- and mass-transfer coefficients will follow the airflow change. If the boards are neatly stacked in the kiln, the new profiles of the coefficients will be mirror images of the old ones (Fig. 2).

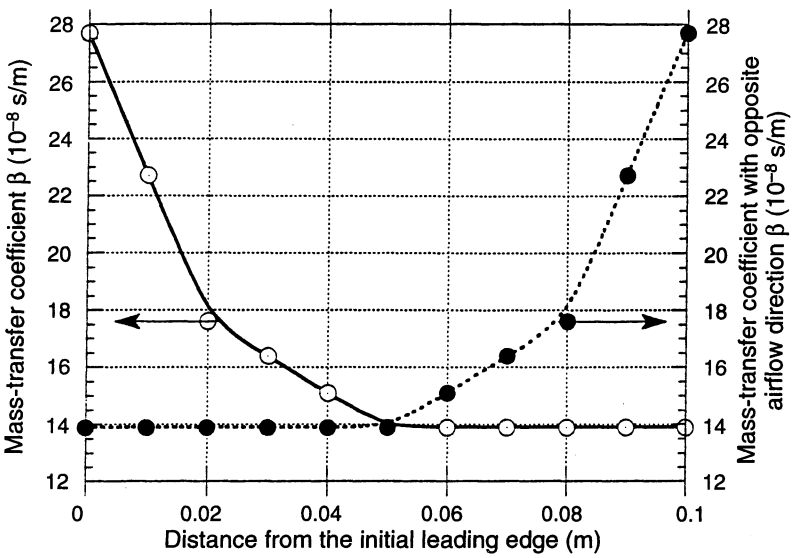

FIG.2–Local external mass-transfer coefficient variation across a single board before and after the air flow is reversed.
Air velocity = 5 m/s. Boards: 100 × 50 mm. Sticker thickness (board gap): 25 mm.

NOMENCLATURE

A coefficient in Equation (12)
B coefficient in Equation (12)
C_p specific heat of moist wood (J/kg·K)
D_b bound-water diffusion coefficient (kg/s·m^3)
E_l effective permeability of wood to liquid flow (s)
E_v effective permeability of wood to water vapour flow (s)
F external mass-transfer coefficient based on molar-concentration difference (mol/m^2·s)
h external heat-transfer coefficient (W/m^2·K)
j_{wb} flux of bound water (kg/m^2·s)
j_{wf} flux of liquid water (kg/m^2·s)
j_{wv} flux of water vapour (kg/m^2·s)
K_v permeability of wood to water vapour (m^2)
K_l liquid permeability of unsaturated wood (m^2)
K_l^s liquid permeability of saturated wood (m^2)
M_v molar mass of water vapour (kg/mol)
P_t total pressure of the air stream (Pa)
p^v vapour pressure (Pa)
$s_{\min}$ minimum saturation for liquid continuity
S entropy (J/mol·K)
T temperature (K)
V specific volume of water vapour (m^3/kg)
X local moisture content (kg/kg)
X_{FSP} moisture content at the fibre saturation point (kg/kg)
$X_{\max}$ moisture content of wood if the entire void structure were filled with liquid (kg/kg)
z space co-ordinate measured normal to the board surface (m)

Greek Characters

ε void fraction
λ thermal conductivity of wood (W/m·K)
μ_b chemical potential of bound water (J/kg)
μ_v chemical potential of water vapour (J/kg)
μ_V viscosity of water vapour (kg/m·s)
ξ distance of the evaporative plane from the surface (m)
ξ_o thickness of the thin dry layer of sapwood (m)
ρ_l density of water (kg/m^3)
ρ_v density of water vapour (kg/m^3)
ρ_s basic density of wood (kg/m^3)
τ time (s)
β external mass-transfer coefficient based on pressure difference (s/m)
δ half thickness of a board (m)

A PHYSICAL MODEL TO SIMULATE THE DRYING OF A SINGLE BOARD

In a previous paper (Pang *et al.* in press), a mathematical model was proposed to simulate the high-temperature drying of *P. radiata* boards. In this model, during the initial stage of drying a heartwood board, an evaporative front is assumed to lie within the wood at which all of the liquid water evaporates. Since the pits are aspirated during the formation of heartwood (Booker 1989), liquid flow is insignificant beneath the front, and thus this evaporative front will withdraw into the material as drying proceeds. The front divides the material into two parts, a wet zone towards the core of the board and a dry zone adjacent to the surface. In the dry zone, moisture exists as bound water and water vapour. Bound water will be in local thermodynamic equilibrium with the water vapour at the local temperature (Stanish *et al.* 1986). In the wet zone, the moisture content remains essentially at the initial value. Once the evaporative front reaches the centre-layer of the board, drying is controlled by bound-water diffusion and water vapour flow.

While the tree is living, the bordered pits are required for transport of liquid nutrients within the sapwood. They subsequently aspirate only as the sapwood dries out. With green sapwood boards, wood cells close to the board's surfaces have been damaged during the milling process and the continuous water column is broken. Therefore, when the sapwood is dried, an evaporative front will appear at a short distance ξ_o from the surface (corresponding to the depth of the layer damaged by sawing). The evaporative front resides at this point for a considerable part of the drying schedule since, at depths greater than ξ_o, most pits are not yet aspirated and sufficient flow of liquid can take place (Fig. 3): capillary tension at the temporarily static evaporative front is sufficient to cause cavitation in the wet interior. The liquid flow towards the evaporative front means that the front will remain at the position ξ_o until the moisture content at the front decreases to the minimum value for liquid continuity. Thenceforward, the front starts to recede into the material and subsequent drying behaviour is similar to that for heartwood drying.

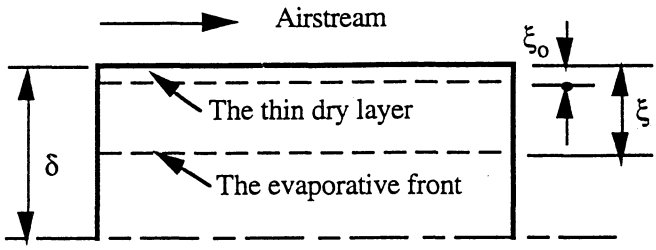

FIG.3–An evaporative front receding in a sapwood board under high-temperature drying.

Heat and Mass Conservation Equations

While heat and moisture mass conservation equations can be applied within a softwood board, the terms in the equations need to be specified separately for the different zones with corresponding boundary and initial conditions. These equations are respectively—

for conservation of heat:

$$C_p \rho_s \frac{\partial T}{\partial \tau} = \frac{\partial}{\partial z}\left[\lambda \frac{\partial T}{\partial z}\right] + \Phi \quad (1)$$

for conservation of moisture:

$$-\rho_s \frac{\partial X}{\partial \tau} = \frac{\partial}{\partial z}(j_{wv} + j_{wf} + j_{wb}) \quad (2)$$

where

C_p is the specific heat of moist wood (J/kg·K)
X is the local moisture content (kg/kg)
ρ_s is the basic density of wood (kg/m^3)
T is the temperature (K)
τ is the time (s)
z is the space co-ordinate measured normal to the board surface (m)
λ is the thermal conductivity of the moist wood (W/m·K)
j_{wv} is the water vapour flux (kg/m^2·s)
j_{wf} is the liquid water flux (kg/m^2·s)
j_{wb} is the flux of bound water (kg/m^2·s)
and Φ is the source term involving the latent heat of vaporisation.

These equations imply that the net transfer processes take place across the grain perpendicular to the airflow direction (this assumption is valid except over small stretches at each end of the board). In the period of drying when the evaporative front is receding into the wood, no liquid water exists in the dry zone; thus, only water vapour and bound-water fluxes will be considered. The same transfer processes will occur within the whole board once the evaporative front reaches the mid-layer of the board. In the wet zone of sapwood the liquid water flow will be taken into account, whereas the vapour and bound-water fluxes can be neglected.

Moisture vapour movement

We assume that the flux of water vapour is proportional to the gradient of the vapour partial pressure, so the vapour flux in the dry zone can be expressed by Darcy's law:

$$j_{wv} = -E_v \frac{\partial p^v}{\partial z} \quad (3)$$

in which E_v is the effective permeability to vapour flow and p^v is the vapour partial pressure. The effective permeability to vapour flow, E_v, may be related to the commonly measured gas permeability, K_v, by the equation:

$$E_v = \frac{K_v \rho_v}{\mu_V} \quad (4)$$

where ρ_v and μ_V are the density and viscosity of the vapour respectively.

The vapour partial pressure can be calculated as a function of local temperature and moisture content using the relationship given by Simpson & Rosen (1981) with some modification for the particular species of wood, *P. radiata* (Pang 1994).

Bound water movement

We use chemical potential as the driving force for bound-water movement. The bound-water flux may be expressed in a form given by Stanish *et al.* (1986):

$$j_{wb} = -D_b(1-\varepsilon)\frac{\partial \mu_b}{\partial z} \quad (5)$$

where μ_b is the chemical potential of bound water, D_b is the bound-water transfer coefficient, and ε is the fractional void space. For local thermodynamic equilibrium, the chemical potential of bound water, μ_b, is the same as that for the vapour, μ_v, and it follows:

$$M_v \frac{\partial \mu_b}{\partial z} = M_v \frac{\partial \mu_v}{\partial z} = -S\frac{\partial T}{\partial z} + V\frac{\partial p^v}{\partial z} \quad (6)$$

The entropy, S, is a state function of temperature and pressure.

When the vapour obeys the Ideal Gas Laws, the above relationship can be transformed into a computable form in which the chemical potential is related to local temperature and pressure gradients (Stanish *et al.* 1986):

$$j_{wb} = -\frac{D_b(1-\varepsilon)}{M_v}\left\{[187 + 35.1 ln\,(\frac{T}{298.15}) - 8.314\, ln\,(\frac{p^v}{298.15})]\frac{\partial T}{\partial z} + 8.314\frac{T}{p^v}\frac{\partial p^v}{\partial z}\right\} \quad (7)$$

Liquid water movement in the wet zone of sapwood

For sapwood, the moisture content is initially high, so when water evaporates at the evaporative front, free water beneath the front will flow towards it because of the liquid pressure gradient. This process can be described by Darcy's law. The pressure gradient in the liquid is assumed to be the consequence of capillary action between the liquid and gas phases within the voids of the wood. Thus we obtain the liquid flux within wood (j_{wf}) as

$$j_{wf} = E_l\frac{\partial p_c}{\partial z} \quad (8)$$

where p_c is the capillary pressure and E_l is the effective permeability to liquid flow, which may also be related to the commonly measured liquid permeability, K_l, by the equation:

$$E_l = \frac{K_l \rho_l}{\mu_l} \quad (9)$$

in which ρ_l and μ_l are the density and viscosity of liquid water respectively. Stanish *et al.* (1986) correlated the liquid permeability (K_l) of unsaturated wood to that measured at saturation (K_l^s) by the expression:

$$K_l = K_l^s\left\{1.0 - cos[\frac{\pi}{2}\frac{(s - s_{\min})}{(1.0 - s_{\min})}]\right\} \quad (10)$$

Here s is the relative saturation of wood defined by

$$s = \frac{\text{Liquid volume}}{\text{Void volume}} = \frac{X - X_{FSP}}{X_{\max} - X_{FSP}} \quad (11)$$

The moisture content at the fibre saturation point is X_{FSP} when the lumens are devoid of any liquid water and $X_{\max}$ is the moisture content of the wood where the entire void structure is filled with liquid. The minimum saturation for liquid flow within the board is $s_{\min}$. When saturation is below this point, unbound water is no longer funicular and the liquid continuity is broken. For softwoods, Spolek & Plumb (1981) assumed that the capillary pressure is a simple algebraic function of saturation:

$$p_c = A\, s^{-B} \quad (12)$$

where A and B are constants.

From Equations (8), (11), and (12), the relationship between liquid water flux and local moisture content becomes:

$$j_{wf} = -\frac{A\,B\,E_l\,(X_{\max} - X_{FSP})^B}{(X - X_{FSP})^{(1+B)}}\,\frac{\partial X}{\partial z} \tag{13}$$

We can use Equations (1) to (13) to predict the temperature, T, and the moisture content, X, in both the dry and the wet zones, the bound water flux (j_{wb}) and the water vapour flux (j_{wv}) in the dry zone, and the liquid water flux in the wet zone (j_{wf}) for sapwood. We can solve the model numerically when the initial and boundary conditions, the various transport coefficients, and the physical properties of wood are known. The method adopted is described elsewhere (Pang 1994; Pang *et al.* in press).

TEMPERATURE AND MOISTURE-CONTENT PROFILES: COMPARISON OF PREDICTED RESULTS WITH EXPERIMENTAL DATA

Drying Tests

A separate experiment was undertaken at New Zealand Forest Research Institute (NZ FRI) drying single boards of sapwood and heartwood under commercial high-temperature conditions. The timber was cut from two *P. radiata* stands, approximately 30 years old, in Kaingaroa Forest. Tests boards were flat-sawn with dimensions of 100 × 50 × 350 mm for sapwood and 100 × 50 × 500 mm for heartwood. Small pieces were cut from each end of the specimens for determination of initial moisture content and basic density.

The specimens for drying were edge- and end-coated twice with a mixture of Altex Devoe Devshield 235 base aluminium paint and converter. In the tests, the specimens were dried in an electrically heated, steam-humidified, tunnel dryer. The dry-bulb/wet-bulb temperatures used were 120°/70°C, 120°/90°C, 140°/70°C, or 140°/90°C and these were controlled automatically with maximum fluctuation of ± 0.5°C. An air velocity of 5 m/s was used in all of the trials.

When the dry-bulb and wet-bulb temperatures were stable, the sample was weighed and placed on the cradle which was hung from a balance on the top of the dryer. Then the data monitor and logger were started to display and to record the elapsed time, temperatures, and sample weight. When all the temperatures at different depths from the drying surface of the board were very close (in a range of 1–2°C) to the dry-bulb temperature, the test was terminated. Finally, the sample was weighed and oven-dried at a temperature of about 103° ± 2°C for 48 hours and the board-average moisture contents were calculated from the oven-dry weight.

For the measurement of local temperatures, four thermocouple holes, 40 mm in length and 2.5 mm in diameter, were drilled into the trailing edge of the specimens. Thermocouples were inserted, a silicon adhesive was pumped in both to seal the holes and to fix the thermocouple tips. The location of the measurement points, 40 mm from the trailing edge, was chosen on the basis that the external mass-transfer coefficients over this region were believed to be relatively constant and could be taken to be representative over the whole board. The four holes were drilled into the trailing edge so that the thermocouples would be approximately 6, 12, 18, and 25 mm below the top face of the board. To measure the surface temperature a slot about 0.5 mm deep was cut with a knife tip and the tip of a thermocouple was pressed into the slot. In these experiments, a dummy board was placed in front of the

sample board so that the mass-transfer coefficients over the sample board could be related to the majority of boards in a kiln stack rather than to the distinctive characteristic of the first board (Fig. 1).

Experimental Results

Wood density and green moisture content

Wood density and green moisture content are two of the most variable properties of wood. For sapwood, the measured density varied from 419 to 488 kg/m^3, and the green moisture content was in the range 1.164 to 1.392 kg/kg. These values agree with data previously reported (Cown *et al.* 1991; Kininmonth & Whitehouse 1991). For heartwood, the density ranged from 372 to 429 kg/m^3 and green moisture content from 0.34 to 0.38 kg/kg. The density of the heartwood was also close to that measured by the above authors, but the moisture content was slightly less than the previously reported values.

Temperature and average moisture-content profiles

The temperature profiles for each test under various external conditions are shown in Fig. 4 and 5 as discrete points. The shapes of these profiles are similar to those reported by Beard *et al.* (1985) for the drying of American yellow poplar (*Liriodendron tulipifera* L.) and Northway (1989) for Australian *P. radiata*. The average moisture content is also plotted.

Heartwood: The test data, external conditions, and values for assumed parameters are given in Fig. 4 and 5, and in Table 1. For heartwood at dry-bulb and wet-bulb temperatures of 120°/70°C (Run 1), the surface temperature rapidly rose above 100°C and increased gradually towards the air temperature with the internal temperatures being close to one other, remaining at about 100°C. Subsequently, the internal temperatures at different depths started to rise as the evaporative front receded into the wood. Finally, the central temperature increased and approached the surface temperature of the board. Unfortunately, in Run 1 the data logger failed to record the sample weight after 7 hours' drying because of a fault in the cradle. By this time, the moisture content had fallen from the initial value of 33.1% to 13.7%.

For Run 4 (120°/90°C), the temperature profile is similar to that of Run 1 (120°/70°C). The moisture content decreased with elapsed time virtually from the beginning of drying except for a short induction period of about 10 minutes. During this time, the board absorbed some moisture from the air and the sample weight increased a little since the surface temperature was below the wet-bulb temperature of the air. However, no constant drying rate period was observed throughout the whole process of drying. In this run the initial moisture content was 32.5%, falling to 11.3% after 7 hours and to 4.0% after 18 hours of drying, at which point drying was terminated.

In the two runs with a dry-bulb temperature of 140°C (140°/70, 140°/90 °C), the surface temperature of the board rose much more rapidly than in those at the lower temperature of 120°C, as expected. Within the first 2 to 3 minutes of the fan and heater being switched on, the surface temperature was over 70°C. The average moisture content dropped also more quickly during drying at 140°C than at the lower air temperature. As expected, for the same dry-bulb temperature, the drying rate with a lower wet-bulb temperature (70°C) was greater than with a higher wet-bulb temperature (90°C). After 12 hours of drying, the moisture contents for Run 3 (140°/70°C) and Run 2 (140°/90°C) were 1.3% and 2.3%

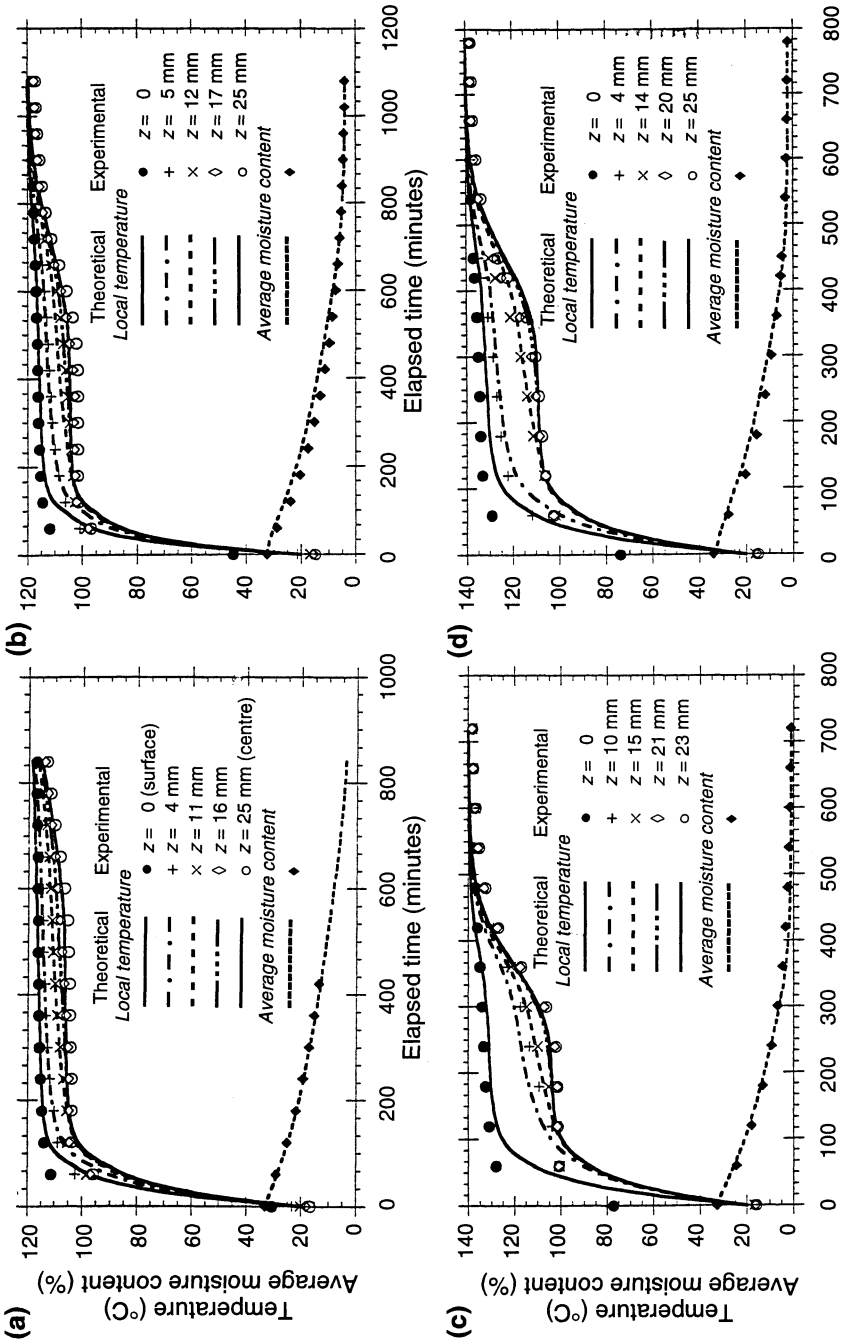

FIG.4–Temperature and moisture-content profiles within a heartwood board: simulation results and comparison with experimental data. Parameter z is the distance from the upper surface of the board. Dry bulb/wet bulb temperatures: (a) 120°/70°C Run 1; (b) 120°/90°C Run 4; (c) 140°/70°C Run 3; (d) 140°/90°C Run 2.

respectively, and the corresponding initial values were 32.9% and 34.2%. By comparison with these final values, the average moisture content for Run 4 (120°/90°C) was still 5.9% after 12 hours, and 4.0% after 18 hours of drying.

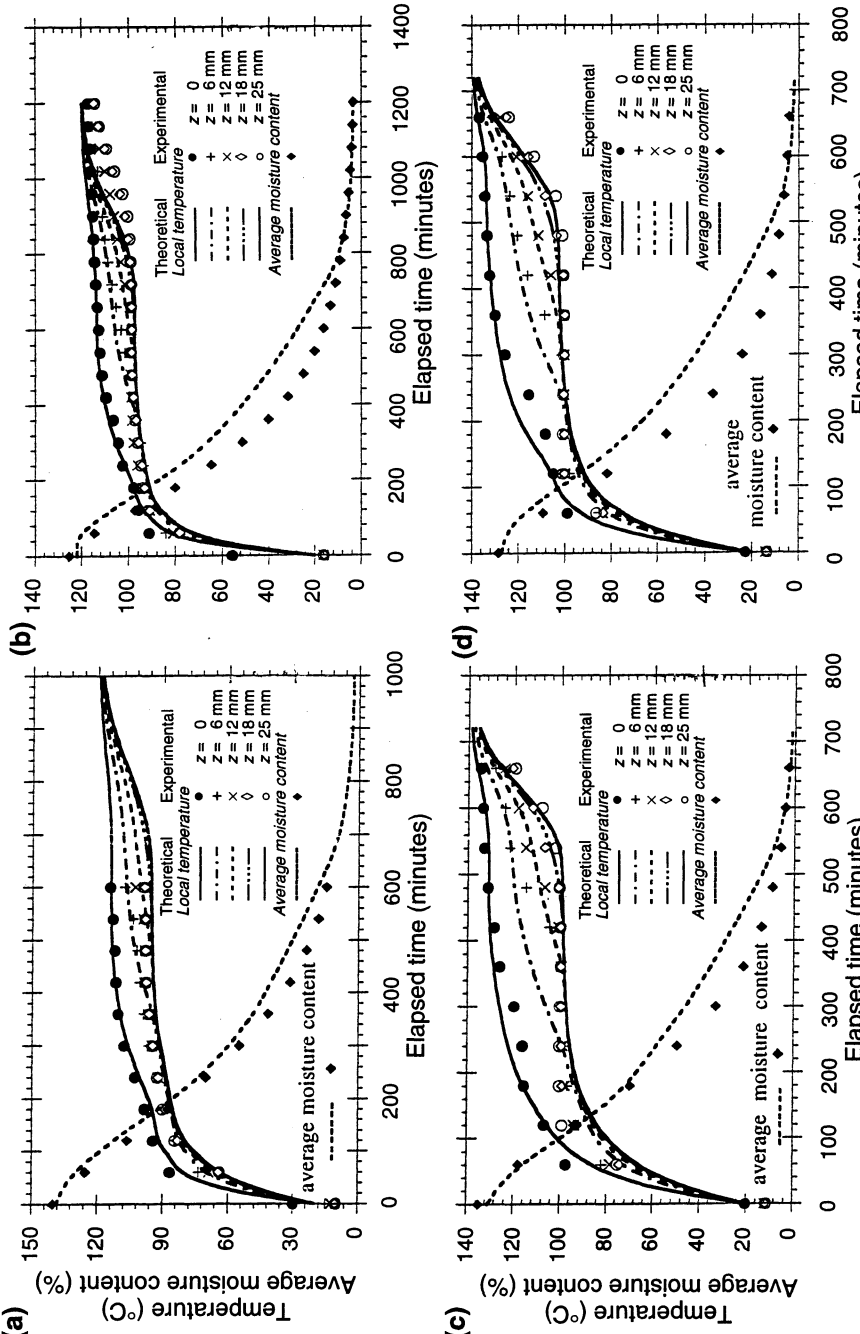

FIG.5–Temperature and moisture-content profiles within a sapwood board: simulation results and comparison with experimental data. Parameter z is the distance from the upper surface of the board. Dry bulb/wet bulb temperatures: (a) 120°/70°C Run 5; (b) 120°/90°C Run 8; (c) 140°/70°C Run 6; (d) 140°/90°C Run 7.

Sapwood: The temperature and average moisture-content profiles for sapwood drying in these tests were similar to those measured by I.Simpson and W.Miller (pers. comm.) and by Northway (1989) for wood from the same species. In the drying experiment for

TABLE 1–Values of the parameters used in the simulation of high-temperature drying of a single *Pinus radiata* board.

Parameters	Heartwood				Sapwood			
	Run 1	Run 4	Run 3	Run 2	Run 5	Run 8	Run 6	Run 7
Dry-bulb/wet-bulb temperatures (°C)	120/70	120/90	140/70	140/90	120/70	120/90	140/70	140/90
Wood permeability to gas, K_G (10^{-15} m^2)	0.2	0.4	0.6	0.5	1.0	1.3	1.2	1.3
Wood permeability to liquid, K_l^s (10^{-16} m^2)	–	–	–	–	14.0	10.0	10.0	14.4
External heat-transfer coefficient, h (W/m^2·K)	30.9	30.9	30.9	30.9	50.0	50.0	50.0	50.0
External mass-transfer coefficient, β (10^{-8} s/m)	16.0	16.0	16.0	16.0	20.0	20.0	20.0	20.0
Thin dry layer thickness, ξ_0 (mm)	–	–	–	–	1.3	1.1	1.1	1.1

sapwood at dry-bulb temperatures of 120°C and 140°C, the surface temperature rose rapidly to above 100°C and then increased slowly towards the air temperature. All of the internal temperatures at different depths (6, 12, 18, and 25 mm beneath the surface) were very similar to each other and remained at about 100°C for a substantial period of time. The length of this period depended on the external conditions: for example, 8 hours for dry-bulb temperature of 120°C, and 5–7 hours for 140°C. During this period the moisture content decreased relatively linearly with drying time, corresponding to a constant drying-rate period. Following this constant drying-rate period, the wood dried in a similar manner to that for heartwood: the drying rate fell and the temperatures at different depths started to increase progressively. Finally, all the temperatures approached the dry-bulb temperature as the moisture contents approached the equilibrium values.

Comparison of Predictions with Experimental Data

Using the mathematical model described in this paper, the temperature and moisture-content profiles within the boards were calculated for each experimental run. The physical properties and parameters were taken as those measured in the experiment or chosen by fitting the predicted temperature and moisture-content profiles to the measured ones (Table 1). The predictions are presented in Fig. 4 and 5 as curves with the experimental data plotted as discrete points to allow comparison between the predictions and the laboratory data.

For heartwood, the predictions matched closely the experimental data for the whole drying process. The discrepancy in moisture content was less than 1% m.c. between the measured and predicted values. The largest difference of 5°C between the predicted and measured temperatures was found in the initial stage of drying, in which the measured surface temperature rose more rapidly than the predicted ones. The internal temperatures started to increase during drying in the same way as those measured.

The features of sapwood drying observed in the tests were predicted from the model. The temperature profiles from the model were in close agreement with the laboratory data. The maximum discrepancy in moisture content between the predictions and the measured data

was found before the evaporative front (in the model) reached the centre layer of the board, with predicted moisture contents being 5~15% m.c. higher than the experimental results. However, the values converged when the drying rate decreased after about 10 hours of drying.

SIMULATION RESULTS BOTH FOR UNIDIRECTIONAL AIRFLOW AND FOR AIRFLOW REVERSALS

Using the values in Table 1 and considering the changes in heat- and mass-transfer coefficients with distance from the leading edge of a board (Fig. 1 and 2), we derived the local temperature and moisture-content profiles across the board at different distances from the leading edge and at different times from our mathematical model with dry bulb/wet bulb temperatures of 120°/70°C. The air velocity was assumed to be 5 m/s. For the airflow reversals, the strategies considered were as follows:

Strategy A: the airflow was reversed every 3 hours;
Strategy B: the airflow was reversed every 4 hours;
Strategy C: the airflow was reversed every 8 hours;
Strategy D: the airflow was reversed only once after 4 hours of drying;
Strategy E: the airflow was reversed once after 2 hours and again after 6 hours of drying.

Strategy A and Strategy B have been practised in commercial kiln drying in New Zealand. Strategy C was used to investigate the influence of extending the interval length for reversing the airflow, while Strategy D and Strategy E were proposed to investigate the effects of only a single reversal or only two reversals.

The changes in the surface and centre temperatures of a sapwood board, the local moisture contents, and the position of the evaporative front are given in Fig. 6 and 7. These variables are given as functions of distance from the original leading edge of the board. In Fig. 6b to 6f, the simulation results are presented for drying after 8 hours with different reversal strategies, compared with those with unidirectional airflow in Fig. 6a. Similar results after 16 hours of drying are shown in Fig. 7. Profiles for heartwood were similar to those for sapwood, but the extent of the changes with distance was less than for sapwood due to the lower initial moisture content of heartwood.

In Figs 6 and 7, the surface and centre temperatures within the wood indicate the overall temperature differences between the surface and the centre-line of the board. Of course, the temperature changes across the thickness of the board were not uniform. In the wet zone, the temperature differences at positions perpendicular to the surface were not significant because the evaporation of water was negligible and the heat requirement for heating up the material was small. Therefore, the temperatures in the wet zone were close to those at the evaporative plane. On the other hand, during the initial period of drying when the wood was relatively cool, the temperature gradients in this wet zone were greatest, but even so the temperature at the centre-line was only about 3°C lower than that at the evaporative plane.

In the dry zone, however, the temperature drop accounted for most of the overall differences in temperature. The quantitative prediction of the temperature distribution was complex owing to the non-linear variation of water vapour flux in this zone. As more water evaporated at a given location (liquid water at the evaporative front and bound-water at other points), more heat was required, resulting in a steeper gradient in temperatures about this

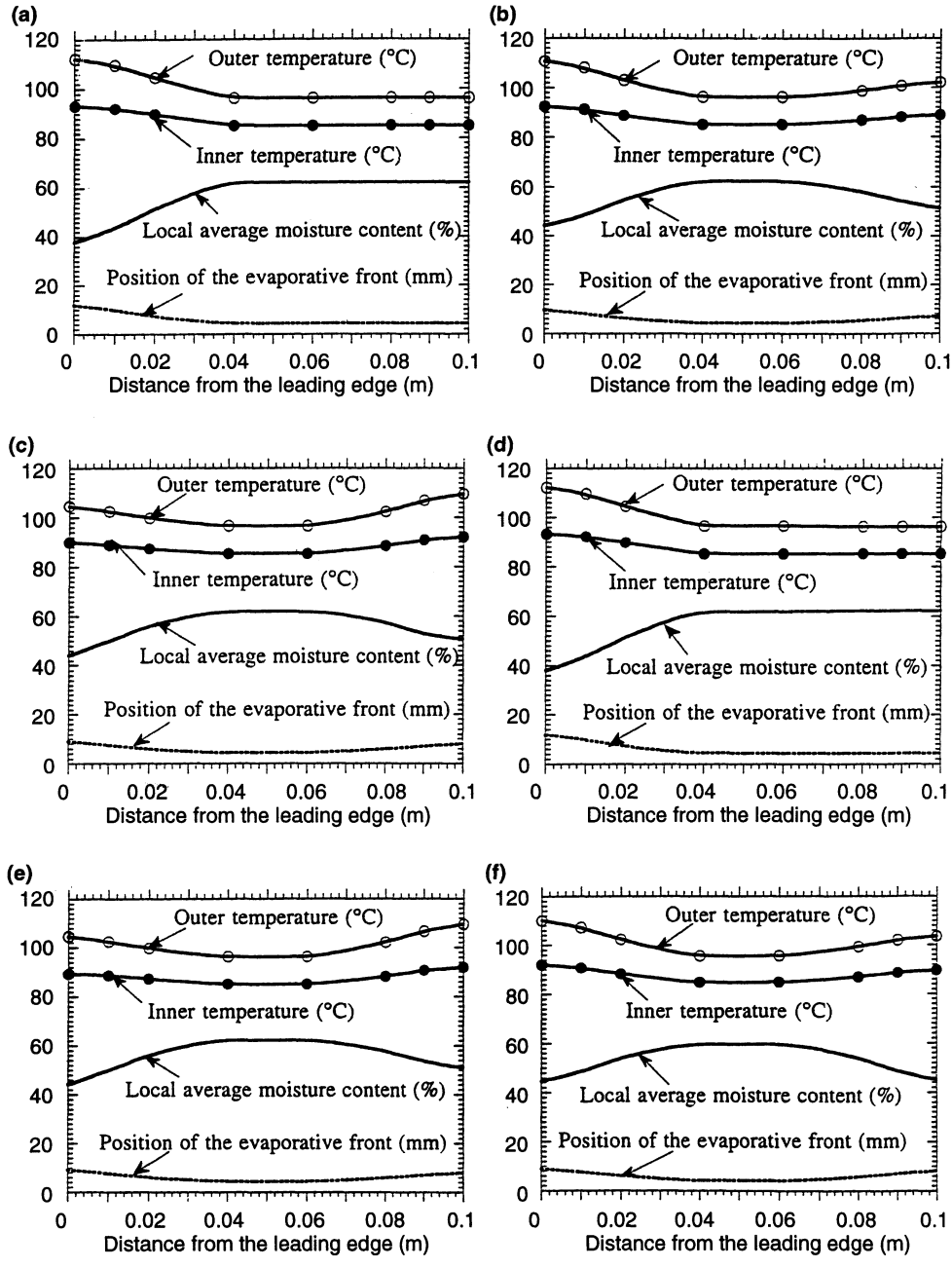

FIG.6–Variations in the surface and centre temperatures, local average moisture content, and the position of the evaporative front with distance along board from the leading edge: sapwood, after 8 hours of drying. Dry-bulb/wet-bulb temperatures: 120°/70°C, air velocity: 5 m/s. (a) Unidirectional airflow; (b) airflow reversed every 3 hours; (c) airflow reversed every 4 hours; (d) airflow reversed every 8 hours; (e) airflow reversed only once after 4 hours; (f) airflow reversed after 2 hours and after 6 hours.

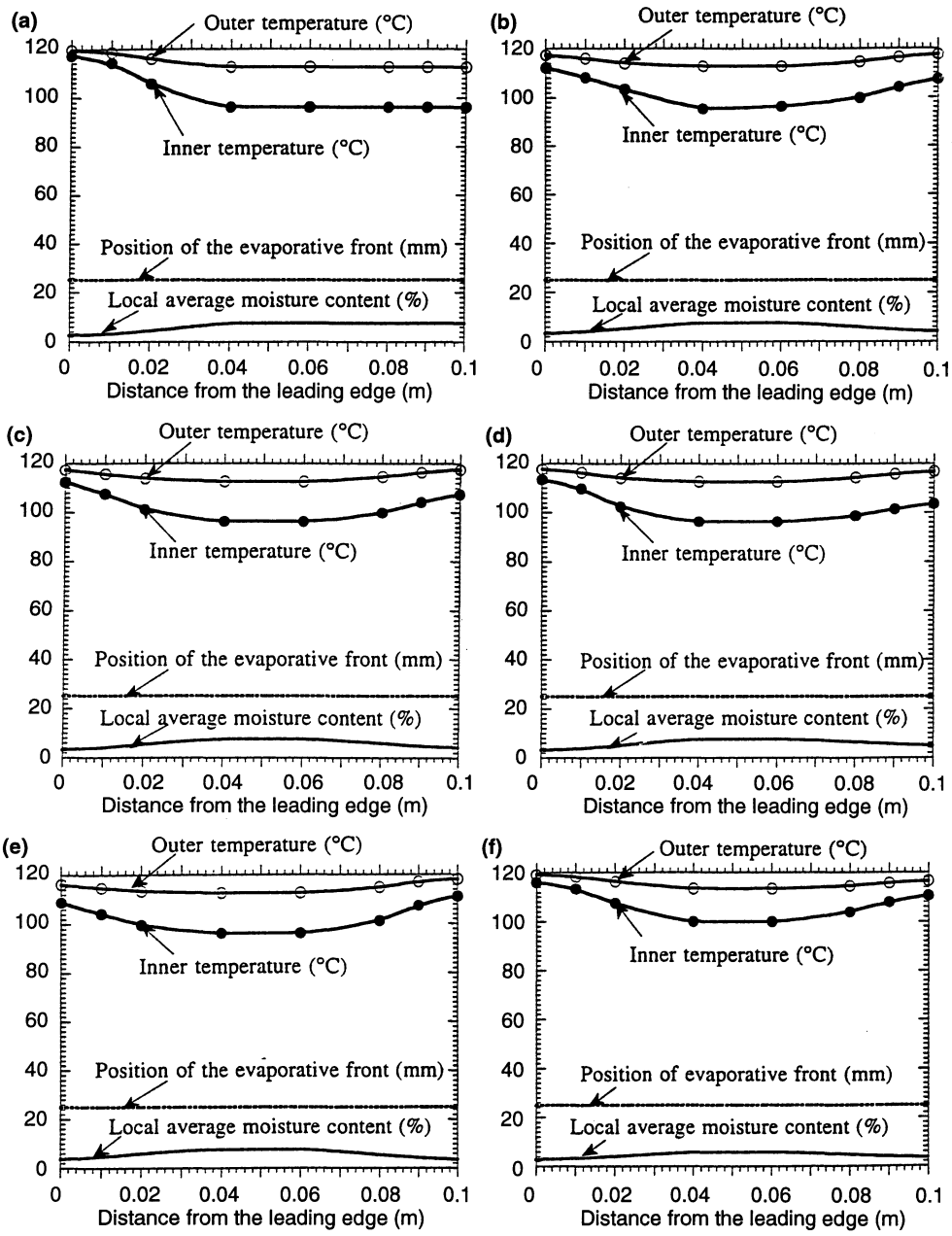

FIG.7–Variations in the surface and centre temperatures, local average moisture content, and the position of the evaporative front with distance along board from the leading edge: sapwood, after 16 hours of drying. Dry-bulb/wet-bulb temperatures: 120°/70°C, air velocity: 5 m/s. (a) Unidirectional airflow; (b) airflow reversed every 3 hours; (c) airflow reversed every 4 hours; (d) airflow reversed every 8 hours; (e) airflow reversed only once after 4 hours; (f) airflow reversed after 2 hours and after 6 hours.

location. Normally, this situation occurs near the timber surface, since all the heat required to heat up the material and to evaporate the moisture (both bound- and unbound-water) is transferred through the external surface.

The local average moisture contents in the board represent some volume-smoothed values at a given position, but the moisture contents varied both with distance from the leading edge and with depth from the board surface. In the dry zone the moisture was in equilibrium with the local temperature of water vapour. At the position just above the evaporative front, the moisture content equalled the fibre saturation value X_{FSP} (about 0.22 kg/kg at boiling point), while near the surface the moisture content decreased from X_{FSP} (when the evaporative front started to recede) towards equilibrium moisture content. The value of equilibrium moisture content at operating conditions of 120°/70°C was about 0.022 kg/kg.

DISCUSSION

Unidirectional Airflow

Sapwood

For sapwood drying with unidirectional airflow (Fig. 6a and 7a), there is an initial period when the liquid flow outwards keeps the evaporative front near the surface for a variable length of time, depending upon the position from the leading edge of the board. The extent of this period of drying depends on both the external heat- and mass-transfer rates and the initial moisture content of the green wood. In the simulation when the initial moisture content was taken as 1.4 kg/kg, this initial period lasted 4 hours for the wood at the leading edge, and in material near the trailing edge of the board this period extended to about 6 hours.

We believe that the appearance of kiln brown stain at a depth of about 1 mm is a practical illustration of the formation of the thin dry layer. Wood sugars and other water-soluble components could migrate to the evaporative front where they undergo reaction to form kiln brown stain.

At the end of the initial period, the evaporative front withdraws into the wood leaving the thin dry layer and, once this occurs, the internal resistance to vapour flow through the wood becomes dominant. Since the wood at the leading edge dries faster and the evaporative front starts to leave the thin dry layer earlier than at other positions, the moisture content at the leading edge drops more quickly (27% m.c. lower than other positions after 4 hours of drying). In subsequent drying, this difference persists until the evaporative front at the leading edge has reached the mid-layer of the board after 12 hours of drying. Thereafter, the moisture content difference is reduced as drying in the driest zone is retarded with only wood cell diffusion taking place. After 16 hours of drying, the difference in local average moisture content is 4% m.c. between the leading edge and the trailing edge. This difference may be further reduced to less than 0.5% m.c. with another 4 hours of drying. A period of 24 hours of drying was recommended by Williams & Kininmonth (1984) for New Zealand *P. radiata* boards of 100 × 50 mm with the schedule considered. However, more recently, shorter drying times have been used commercially by employing air velocities than higher 5 m/s in the kiln.

The greatest difference in surface temperature across the board also occurs between the leading edge and the trailing edge, with a value of 25°C after 6 hours of drying. This difference falls to 16°C after 8 hours and to 7°C after 16 hours of drying.

The inner temperatures everywhere are similar to each other, with a difference of 5°C before the evaporative front at the leading edge has reached the centre-line of the board. Thenceforth, the centre temperature at the leading edge starts to rise while the centre temperatures at other positions remain at around boiling point (100°C). The largest difference of 20°C in inner temperature occurs after 16 hours of drying when the evaporative front near the trailing edge has just reached the centre-line of the board. The differences for both surface and inner temperatures are reduced to less than 3°C after 20 hours of drying.

Heartwood

The above features of sapwood drying with unidirectional airflow also apply to heartwood, except that for heartwood drying the evaporative front withdraws continuously into the material virtually from the start of drying (Pang *et al.* in press). During this period of drying, at positions near the leading edge the temperatures rise more swiftly, the evaporative front recedes more deeply, and the average moisture contents decrease more quickly than at other positions across the board in the airflow direction. After 4 hours of drying, the temperature near the leading edge begins to rise slowly due to loss of moisture at the surface and the mass-transfer rate falls. After 12 hours, the evaporative front everywhere reaches the board's centre-line. At this time, the moisture content at the surface is virtually at equilibrium value and the surface temperature approaches the dry-bulb temperature of the air. In subsequent drying, the heat- and mass-transfer rates at any point become much lower than those in the initial period of drying, and the differences in temperatures and average moisture contents across the board finally become insignificant.

For heartwood drying, the largest temperature difference occurs on the surfaces between the leading edge and the trailing edge with a value of about 10°C after 2 hours' drying, while after 12 hours the surface temperature at the trailing edge is only 5°C lower than that at the leading edge. This temperature difference decreases to only 0.1°C after 20 hours of drying.

The moisture content at the leading edge of a heartwood board is lower than that close to the trailing edge of the board. The moisture-content difference across the board is much smaller than that for sapwood, remaining about 3% m.c. in first 12 hours of drying, and is due mainly to the variation in depth of the evaporative plane at various positions across the board. The moisture content in the dry zone is lower than that in the wet zone. During the final period of drying after 12 hours, this moisture-content variation is reduced, becoming insignificant after 20 hours of drying.

Airflow Reversals

From the simulation results it can be seen that, when the airflow is reversed, the previous leading edge becomes the trailing edge and vice versa. Correspondingly, the heat- and mass-transfer coefficient profiles are reversed. The temperature and moisture-content profiles will now track these changes. However, before the first change in the flow direction, the temperature and moisture content profiles are the same as those with unidirectional airflow, as discussed in the previous section.

For sapwood, the most non-uniform profiles of temperature and average moisture content occur between 4 and 12 hours of drying with unidirectional airflow. However, when the fan direction is changed every 4 hours in a kiln, the differences in temperature and moisture

content can be reduced greatly some time after the first flow reversal. Just before the airflow is reversed (after 4 h), the surface temperature at the leading edge is 14°C higher and the moisture content there is 27% lower than the corresponding values near the trailing edge. After the airflow has been reversed once, these differences fall to 8°C for the temperature and 13% for the average moisture content. With another 4 hours drying (after 8 hours from the start), the temperatures at positions near both ends are quite similar, but higher than those in the middle area of the board (Fig. 6c). Likewise, the moisture-content profiles at both ends are similar, but lower than those in the middle area. This feature persists, even with continuing airflow reversals (Fig. 7c). The lower temperatures and the higher moisture contents in the middle-area are due to the lower average external heat- and mass-transfer rates even though the airflow has been reversed several times. The reason for this persistence lies in the fact that the airflow reversals influence only the magnitude of the transfer coefficients at the leading and trailing edges of each board. The drying conditions across the central strip of the board are barely changed. The final differences in temperature and average moisture content are 3°C and 1% m.c. respectively after 20 hours of drying.

In a sapwood board that is being dried with airflow reversals every 8 hours, there are large temperature gradients across the board and a wide variation in moisture content before the airflow direction is changed (Fig. 6d). However, with a single fan reversal at 8 hours, the variation in these profiles with distance across the board is reduced and similar profiles to those for airflow reversals every 4 hours can be achieved after 16 hours (Fig. 7d).

With only one airflow reversal after 4 hours, similar profiles of local temperature and moisture-content to those with reversals every 4 hours have been observed after 8 hours and 16 hours of drying. Hence, further reversals are of only marginal benefit (Fig. 6e and 7e). However, this conclusion is valid only for the drying of a single board. In kiln-wide drying, the single reversal may introduce some differences when the changes in external conditions across the whole stack are taken into consideration.

An advantage of reversing the airflow every 3 hours is the reduction in the maximum differences in moisture content and temperatures since the first reversal takes place before the greatest differences are generated with unidirectional airflow. The largest difference in moisture content becomes 20% between 3 and 10 hours of drying. The maximum differences in surface and inner temperatures are 15°C after 8 hours and 16°C after 16 hours respectively. The final result is similar to that with airflow reversals every 4 hours, after 16 hours of drying (Fig. 7), but stress development is likely to be less severe as the maximum moisture-content difference is reduced in the early stage of drying.

The maximum moisture-content difference across a single board during the early stage of drying should be further reduced by reversing the airflow for the first time after 2 hours. Under these conditions, the maximum difference in moisture content is 16% m.c. after 4 hours of drying. A second reversal after 6 hours from start of drying, produces similar moisture-content profiles in the final period of drying (Fig. 6f and 7f).

For the drying of heartwood, airflow reversals also change the profiles of temperature and local average moisture content within a board, but the benefit is not as significant as for sapwood because of the much lower initial moisture content in heartwood. Details of simulation results with airflow reversals for heartwood have been published elsewhere (Pang *et al.* 1992).

CONCLUSIONS

The mathematical model proposed is based on the physical features of wood and on observed drying characteristics, distinguishing between sapwood and heartwood. Existence of the receding evaporative front in both sapwood and heartwood boards, and formation of the thin dry layer at the surface in sapwood boards are believed to describe the general behaviour of softwood boards when dried at high temperatures.

From the proposed mathematical model, we can predict the variations of local temperature and moisture content with depth of the board in drying of a *P. radiata* board by using the mean mass-transfer coefficients measured by Kho *et al.* (1989, 1990). The predictions closely match the laboratory experimental data for drying a single board, giving some further confidence in extending the model to drying when variations in mass-transfer coefficients are taken into account.

When the air flows in only one direction, the temperatures are higher and the moisture contents are lower at the leading edge than in other positions downstream owing to the decrease in the external heat- and mass-transfer rates across the board. These differences can be reduced by reversing the airflow. Airflow reversals every 4 or 8 hours can lessen the maximum moisture-content difference, but the greatest value cannot be reduced. Reversing the airflow twice, after 2 and 6 hours, is more effective in limiting the moisture-content difference in the airflow direction. This should reduce the number of drying defects. However, various strategies considered for the airflow reversals produce essentially similar temperature and moisture-content profiles in the final period of drying (after 16 hours).

We believe that the proposed mathematical model offers an accurate description of transfer processes within wood during high-temperature drying; thus, this model can be applied to analyse the drying behaviour through a kiln-stack of boards. From such analysis, the influence of airflow reversals on kiln-scale drying can be carried out (Pang *et al.* 1994).

ACKNOWLEDGMENTS

This work was supported by the New Zealand Public Good Science Fund (UOC 302 and 406). Pang Shusheng also acknowledges financial support from New Zealand FRST fund (CO4415) in preparing this paper. The single-board experiments were carried out at the New Zealand Forest Research Institute, Rotorua. The authors wish to thank Mr W.R.Miller, Mr A.N.Haslett, and Mr I.G.Simpson for the arrangement and for their help in conducting the drying tests. We also appreciate the helpful discussions with Dr J.A.Kininmonth of Windsor Engineering Group Ltd, Rotorua, in preparing this paper.

REFERENCES

ASHWORTH, J.A. 1977: The mathematical simulation of the batch drying of softwood timber. Ph.D. Thesis, University of Canterbury, New Zealand.

BEARD, J.N.; ROSEN, H.N.; ADESANYA, B.A. 1985: Temperature distribution in lumber during impingement drying. *Wood Science and Technology 19*: 277–86.

BOOKER, R. E. 1989: Hypothesis to explain the characteristic appearance of aspirated pits. Pp.1–8 *in* Second Pacific Regional Wood Anatomy Conference, Forest Products Research and Development Institute, Los Banos (College), Laguna, Philippines, 15–21 October.

BOOKER, R.E.; HASLETT, A.N. 1993: Wood vibrations: Putting a stop to bad checks. *New Zealand Forest Industries 24(11)*: 27–30.

COWN, D.J.; McCONCHIE, D. L.; YOUNG, G.S. 1991: Radiata pine wood properties survey (1977-1982). *New Zealand Ministry of Forestry, Forest Research Institute, FRI Bulletin No.50* (rev.).

KHO, P.C.S.; KEEY, R.B.; WALKER, J.C.F. 1989: Effect of minor board irregularities and air flows on the drying rate of softwood timber board in kilns. *Proceedings of Second IUFRO International Wood Drying Symposium, Seattle*: 150–7.

———1990: The variation of local mass-transfer coefficients in streamwise direction over a series of in-line, blunt slabs. *Proceedings of Chemeca'90 Conference, Auckland, New Zealand, 1*: 348–55.

KININMONTH, J.A.; WHITEHOUSE, L.J. 1991: "Properties and Uses of New Zealand Radiata Pine: Volume 1—Wood Properties". New Zealand Ministry of Forestry, Forest Research Institute, Rotorua, New Zealand.

LANGRISH, T.A.G.; KEEY, R.B.; KHO, P.C.S.; WALKER, J.C.F. 1993: Time-dependent flow in arrays of timber boards: Flow visualisation, mass-transfer measurement and numerical simulation. *Chemical Engineering Science 48*: 2211–23.

LEE, H.S. 1990. Flow visualization on high temperature wood drying. B.E. Report (Chemical and Process Engineering), University of Canterbury, Christchurch, New Zealand.

MILLER, W.R. 1972: Mass-transfer within arrays. B.E. Report (Chemical Engineering), University of Canterbury, Christchurch, New Zealand.

NORTHWAY, R. 1989: Moisture profiles and wood temperature during very high-temperature drying of *Pinus radiata* explain lack of degrade. *Proceedings of Second IUFRO International Wood Drying Symposium, Seattle*: 24–8.

PANG SHUSHENG 1994: High-temperature drying of *Pinus radiata* boards in a batch kiln. Ph.D. Thesis, University of Canterbury, Christchurch, New Zealand.

PANG SHUSHENG; KEEY, R.B.; LANGRISH, T.A.G. 1992: The influence of airflow reversals during the high temperature kiln drying of *Pinus radiata* boards. *Proceedings of Chemeca'92, Canberra, Australia, 2*: 153–60.

PANG SHUSHENG; LANGRISH, T.A.G.; KEEY, R.B.: Moisture movement in softwood timber at elevated temperatures. *Drying Technology 14(7)* (in press)

PANG SHUSHENG; KEEY, R.B.; WALKER, J.C.F.; LANGRISH, T.A.G. 1994: Airflow reversals in high-temperature kiln drying of *Pinus radiata* boards. 2: Drying of a stack of boards. *New Zealand Journal of Forestry Science 24(1)*: 104–19.

SIMPSON, W.T.; ROSEN, H.N. 1981: Equilibrium moisture content of wood at high temperatures. *Wood and Fibre 13(3)*: 150–8.

SØRENSEN, A. 1969: Mass-transfer coefficients on truncated slabs. *Chemical Engineering Science 24*: 1445–60.

SPOLEK, G.A.; PLUMB, O.A. 1981: Capillary pressure in softwood. *Wood Science and Technology (15)*: 189–99.

STANISH, M.A.; SCHAJER, G.S.; KAYIHAN, F. 1986: A mathematical model of drying for hygroscopic porous media. *AIChE Journal 32(8)*: 1301–11.

WILLIAMS, D.H.; KININMONTH, J.A. 1984: High temperature kiln drying of radiata pine sawn timber. *New Zealand Forest Service, Forest Research Institute, FRI Bulletin No.73.*